Uncertainties in Profiler and Polarimetric DSD Estimates and Their Relation to Rainfall Uncertainties

CHRISTOPHER R. WILLIAMS

Cooperative Institute for Research in Environmental Sciences, University of Colorado, and NOAA/Earth System Research Laboratory, Boulder, Colorado

PETER T. MAY

Bureau of Meteorology Research Centre, Melbourne, Victoria, Australia

(Manuscript received 18 June 2007, in final form 18 March 2008)

ABSTRACT

Polarimetric weather radars offer the promise of accurate rainfall measurements by including polarimetric measurements in rainfall estimation algorithms. Questions still remain on how accurately polarimetric measurements represent the parameters of the raindrop size distribution (DSD). In particular, this study propagates polarimetric radar measurement uncertainties through a power-law median raindrop diameter D_0 algorithm to quantify the statistical uncertainties of the power-law regression. For this study, the power-law statistical uncertainty of D_0 ranged from 0.11 to 0.17 mm. Also, the polarimetric scanning radar D_0 estimates were compared with the median raindrop diameters retrieved from two vertically pointing profilers observing the same radar volume as the scanning radar. Based on over 900 observations, the standard deviation of the differences between the two radar estimates was approximately 0.16 mm. Thus, propagating polarimetric measurement uncertainties through D_0 power-law regressions is comparable to uncertainties between polarimeteric and profiler D_0 estimates.

1. Introduction

One major application of polarimetric weather radar is to improve surface rainfall estimation by quantifying the vertical and spatial distribution of the raindrop size distribution (DSD) in all regions of the precipitation cloud system. The polarimetric measurements of reflectivity, differential reflectivity, and specific differential phase are used in algorithms to estimate integrated quantities of the DSD, including the median volume-weighted raindrop diameter D_0, which divides the total volume of liquid water into two equation portions. Some assumptions or measurements of D_0 are implied in almost all radar estimates of rainfall.

Given that rain gauges have small sample volumes relative to radar pulse volumes and that radars measure the precipitation several kilometers above the ground as well as DSD dependencies for Z–R relations, it is not unusual to have differences on the order of 100% in storm rainfall accumulations between surface rain gauge and radar estimates (Brandes et al. 1999). Verifying radar-derived quantities using surface instruments is always complicated by the physical separation and sample volume mismatches between gauges and radars (Williams et al. 2000). Therefore, this study compares D_0 estimates in approximately the same radar pulse volume but using a side-looking polarimetric radar and vertically pointing profiling radars using different radar methodologies to estimate the median raindrop diameter. This experiment design also avoids time and space evolutions of the DSD as the raindrops fall from the altitude of the radar observations down to the surface gauge.

Using an exponential DSD and a linear raindrop axis ratio, the median volume diameter can be expressed as a linear function of differential reflectivity (Seliga and

Corresponding author address: Christopher Williams, Mail Stop R/PSD2, 325 Broadway, Boulder, CO 80305.
E-mail: christopher.williams@colorado.edu

DOI: 10.1175/2008JTECHA1038.1

Bringi 1976). When the DSD deviates from an exponential shape, as with a modified gamma form (Ulbrich 1983), and the raindrop axis ratios deviate from a linear function, a power-law regression of the form $D_0 = aZ_{\rm dr}^b$ is the simplest algorithm to estimate the median raindrop diameter D_0 from polarimetric scanning radar measurements (Bringi et al. 2002; Gorgucci et al. 2002). The differential reflectivity $Z_{\rm dr}$ is the ratio of horizontal to vertical polarized reflectivity, and its interpretation depends on the assumed oblateness relationship of the raindrops as they increase in diameter (Keenan et al. 2001; Brandes et al. 2004b). Note that the power-law regression is independent of reflectivity magnitude and is only dependent on the ratio of the horizontal to vertical polarized reflectivities.

The Doppler velocity reflectivity spectra from vertically pointing radar wind profilers operating at 50 and 920 MHz can be processed to retrieve the vertical air motion and the raindrop size distribution at all range gates below the freezing level (Rajopadhyaya et al. 1998). Since the shape of the retrieved raindrop size distribution is dependent on the shape of the observed Doppler velocity spectrum, the profiler-derived D_0 estimate is independent of the reflectivity magnitude (Williams 2002). Thus, both the polarimetric and profiler retrieval methodologies are indirect measurements of D_0, and the methodologies are independent of reflectivity.

The polarimetric and profiler estimates of D_0 have retrieval uncertainties, and the variance of the difference between the two D_0 estimates will always be greater than the sum of the polarimetric and profiler retrieval variances because of 1) the retrieval uncertainties of both radar methodologies, 2) the spatial variability of the precipitation in the mismatched radar volumes, and 3) the temporal evolution of the precipitation during the radar dwell time.

This study builds off of the work of May et al. (2001) and May and Keenan (2005) and uses the same instruments but different rain events. This short note focuses on the statistical uncertainty of a power-law D_0–$Z_{\rm dr}$ relationship due to the measurement uncertainty of $Z_{\rm dr}$ and compares these power-law uncertainties with vertically pointing radar wind profiler D_0 retrieved uncertainties. The methodology presented here should be included in studies using larger datasets investigating D_0–$Z_{\rm dr}$ relationships in different rain regimes and meteorological conditions.

This note has the following structure. Section 2 estimates the polarimetric differential reflectivity uncertainty and the profiler D_0 uncertainty. Section 3 propagates the polarimetric measurement uncertainties through a D_0 power-law regression. Section 4 compares the profiler-retrieved D_0 with the observed polarimetric $Z_{\rm dr}$, and the concluding remarks are presented in section 5.

2. Radar measurement uncertainties

In this study, the C-band polarimetric scanning radar (CPOL) operating near Darwin, Australia, made range–height indicator (RHI) scans over two vertically pointing profiling radars operating at 920 and 50 MHz located 24 km away from CPOL (May et al. 2001). The CPOL reflectivity and differential reflectivity measurement uncertainties and the profiler median raindrop diameter retrieval uncertainties are presented in this section.

a. Polarimetric radar measurement uncertainties

During RHI scans directed over the profilers, the CPOL radar transmitted alternating horizontal- and vertical-polarized pulses with 64 consecutive horizontal and vertical pulse-pairs processed to estimate the reflectivity at horizontal and vertical polarizations, the differential reflectivity, the specific differential phase, and the correlation between the vertical- and horizontal-polarized voltages at zero time lag for each 250-m range gate (Keenan et al. 1998; May and Keenan 2005). The horizontal and vertical reflectivity can be expressed in linear units, z_h and z_v (mm^6 m^{-3}), and in decibel units (dBZ) using $Z_h = 10\log(z_h)$ and $Z_v = 10\log(z_v)$.

The reflectivity measurement uncertainty is related to the correlation of the 64 radar pulses used to generate each reflectivity estimate. If the return from each radar pulse were uncorrelated with the other pulses, then the variance of the estimated horizontal reflectivity would be $\mathrm{var}(z_h) = z_h^2/64$. Because the samples are correlated, however, the variance is dependent on the correlation coefficient $\rho_{z_h}(k)$ between the complex signal samples at different lag k and can be expressed as (Bringi and Chandrasekar 2001)

$$\mathrm{var}(z_h) = \sigma(z_h)^2 = \frac{z_h^2}{N}\sum_{k=-(N-1)}^{(N-1)}\left(1 - \frac{|k|}{N}\right)|\rho_{z_h}(2k)|, \tag{1}$$

where N is the total number of signal samples and the index $2k$ accounts for 2 times the lag due to the alternating pulse polarity. If the Doppler spectrum of the horizontal reflectivity can be described by a Gaussian shape with mean velocity $\bar{v}$ and spread σ_v, then the correlation coefficient at lag k can be estimated from the autocorrelation function using

$$|\rho_{z_h}(k)| = \left[\exp\left(-\frac{8\pi^2\sigma_v^2 k^2 T_s^2}{\lambda^2}\right)\right]^2, k = 0, 1, 2, \ldots, 2N, \quad (2)$$

where T_s is the sampling interval, λ is the radar operating wavelength, the squared term on the right-hand side of (2) is because the autocorrelation function is derived from the complex signal voltages, and ρ_{z_h} is related to the power of the signal with $|\rho_{\text{power}}| = |\rho_{\text{voltage}}|^2$.

While (1) estimates the variance of z_h in linear units, the variance of Z_h in decibel units is estimated using perturbation analysis on the nonlinear log function and is given as (Bringi and Chandrasekar 2001; Doviak and Zrnic 1993)

$$\text{var}(Z_h) = \sigma(Z_h)^2 = \left[10\log\left(1 + \frac{\sigma_{z_h}}{z_h}\right)\right]^2. \quad (3)$$

The differential reflectivity can be expressed in linear (z_{dr}) and decibel (Z_{dr}) units and is estimated from the horizontal and vertical polarization reflectivity estimates using (Doviak and Zrnic 1993)

$$z_{\text{dr}} = z_h/z_v(\text{unitless}) \quad \text{and} \quad (4a)$$

$$Z_{\text{dr}} = 10\log(z_h/z_v) = 10\log(z_{\text{dr}})\ (dB). \quad (4b)$$

The z_{dr} variance is dependent on the variances of z_h and z_v, as well as the correlation between z_h and z_v during the N samples used to estimate z_{dr}. Random variable perturbation analysis of z_h/z_v indicates that the variance of z_{dr} is given by the expression (Bringi and Chandrasekar 2001)

$$\text{var}(z_h/z_v) = \sigma(z_h/z_v)^2 = 2(z_h/z_v)^2 \frac{1}{N}\sum_{k=-(N-1)}^{(N-1)}\left(1 - \frac{|k|}{N}\right)[|\rho_{z_h}(2k)| - |\rho_{hv}(0)|^2|\rho_{z_h}(2k+1)|], \quad (5)$$

where $\rho_{hv}(0)$ is the correlation coefficient of the horizontal and vertical polarized voltages at zero lag, and it is assumed that $\rho_{z_h}(k)=\rho_{z_v}(k)$. Note that even if all of the raindrops were spherical and $z_h = z_v$, $\text{var}(z_h/z_v)$ would still be greater than zero because of the summation of the correlation coefficients at different lags. Similar to (3), the variance of Z_{dr} is found using perturbation analysis of the log function to yield

$$\text{var}(Z_{\text{dr}}) = \sigma(Z_{\text{dr}})^2 = \left[10\log\left(1 + \frac{\sigma_{z_{\text{dr}}}}{z_{\text{dr}}}\right)\right]^2. \quad (6)$$

To provide reference values of measurement uncertainties for this study, the Doppler spectrum spreads of 1 and 2 m s^{-1} result in reflectivity measurement uncertainties of $\sigma(Z_h) = 0.9$ and 0.7 dBZ. Larger Doppler spectrum spreads lead to smaller uncertainties because the correlation coefficient decreases faster in (2) with increasing spread σ_v. Using Doppler spectrum spreads of 1 and 2 m s^{-1} and a correlation coefficient at zero lag of $\rho_{hv}(0) = 0.97$ results in differential reflectivity uncertainties of $\sigma(Z_{\text{dr}}) = 0.34$ and 0.25 dB. Again, larger spectrum spread (2 m s^{-1}) corresponds to smaller uncertainties. Increasing the correlation coefficient at zero lag to $\rho_{hv}(0) = 0.99$ results in $\sigma(Z_{\text{dr}}) = 0.21$ and 0.15 dB for spectrum spreads of 1 and 2 m s^{-1}, respectively. It is interesting to examine (1) and (5) with regard to the number of radar samples used in the estimate. If $N = 1$, the uncertainties of z_h and z_{dr} have the same order of magnitude as z_h and z_{dr} ($\sigma_{Z_h} \sim 3$ dBZ and $\sigma_{Z_{\text{dr}}} \sim 4.8$ dBZ). As N increases, the uncertainties of z_h and z_{dr} decrease but at a rate dependent on the correlation between the complex signal samples. Thus, this is the mathematical background describing how the measurement uncertainty decreases as more samples are processed so that the radar measurements can be used for meteorological applications.

b. Profiler DSD parameter uncertainty

The two profiling radars used in this study operated at 50 and 920 MHz and estimated the Doppler velocity spectrum due to Bragg scattering resulting from changes in the turbulent refractive index (Gage et al. 1999) and to Rayleigh scattering from the hydrometeors (Gossard 1988; Ralph 1995). The two profilers had different sensitivities to the Bragg and Rayleigh scattering processes and, in this study, a least squares minimized Gaussian function was determined for each 50-MHz profiler spectrum to estimate the mean vertical air motion and the turbulent spectrum broadening. Each spectrum was visually inspected, and the minimum and maximum velocities used in the fit were manually adjusted if needed so that the Gaussian function was centered on the Bragg-scattering portion of the Doppler velocity spectrum. The raindrop size distribution was estimated at each range gate by first shifting the observed 920-MHz Doppler velocity spectra by the 50-MHz profiler-estimated vertical air motion. Then, the spectral broadening of the shifted terminal fall speed spectra was removed using the deconvolution modeling method (Lucas et al. 2004; Schafer et al. 2002) to provide the DSD estimate. Last, the median raindrop di-

ameters from 1.7 to 4 km above the ground were estimated from each retrieved DSD.

One of the technical challenges in retrieving the DSD from vertically pointing radars is to fully deconvolve the broadening effects in the recorded reflectivity-weighted Doppler velocity spectra due to the radar finite antenna beamwidth. The spectral broadening effects increase as the turbulence, horizontal wind magnitude, and wind shear magnitude increase in the radar pulse volume. As discussed in Rajopadhyaya et al. (1998), the difference in beam-broadening effects for the 50- and 920-MHz profilers due to the 3° versus 9° beamwidths is not significant for low wind speeds or when the turbulent broadening is significantly larger than beam broadening (i.e., $|v|$ is small or σ_v is large).

Another factor that is considered in retrieving the DSD is that finite noise in the Doppler velocity spectrum prohibits the complete deconvolution of the finite beam-broadening effect, resulting in overestimates of reflectivity in the tails of the spectrum at small and large drop sizes. Because of the sixth-power scaling of reflectivity with diameter, these overestimates result in the retrieval of more smaller drops and lead to a potential low bias of D_0. This bias has been minimized by limiting the minimum resolvable drop size to ~0.7 mm.

Several studies have addressed the complex issues of deriving the DSD from vertically pointing radar observations to account for the vertical air motion, the spectral broadening of the recorded Doppler velocity spectra, and the underlying assumption that the DSDs are stationary during the radar dwell time (Wagasugi et al. 1986; Sato et al. 1990; Rajopadhyaya et al. 1999; Schafer et al. 2002). The uncertainties of these factors all contribute to the uncertainties of the estimated DSD. In this study, we do not want to quantify the uncertainties of each factor but rather rely on the results of previous studies using simulated data to characterize the statistical properties of the DSD uncertainties. One of the most comprehensive of these studies is by Schafer et al. (2002).

From the results of Schafer et al. (2002) we can see several trends. First, as the clear air spectral width increases, the error in the estimated DSD increases dramatically. However, there is also a dependence on the underlying DSD. To first order, this dependency is related to the median volume diameter, D_0. The largest errors are associated with small and large D_0 values, while the smallest errors are associated with D_0 between 1 and 2.5 mm. These limits arise because for small D_0, the raindrop fall speeds collapse into a narrow velocity range near the Bragg scattering air motion peak, causing difficult retrievals. For very large D_0, the fall speeds of the large drops approach a constant value as the raindrop diameter increases.

TABLE 1. Standard deviation (mm) of retrieved D_0 as functions of the air motion spectral width and the value of D_0 as estimated from Figs. 2–4 of Schafer et al. (2002).

	Air motion spectral width		
Retrieved D_0	0.5 m s^{-1}	1.5 m s^{-1}	3.0 m s^{-1}
1 mm	0.1	0.2	0.3
2 mm	0.25	0.3	0.5

From Figs. 2–4 of Schafer et al. (2002), we can estimate the uncertainty of the retrieved D_0 as functions of air motion spectral width and the retrieved value of D_0. Table 1 shows the standard deviation of the retrieved D_0 for air motion spectral widths ranging from 0.5 to 3.0 m s^{-1} and for D_0 ranging from 1 to 2 mm. During extreme spectral broadening events, $\sigma(D_0)$ approaches 0.5 mm. During stratiform rain, the spectral width is typically less than 0.5 m s^{-1}, and the uncertainty is expected to be less than 0.25 mm for all values of D_0. There may be other contributions to differences and errors in D_0 measurements due to the time variation of D_0 during the profiler data acquisition, as discussed by May et al. 2001.

3. Statistical uncertainties in the power-law D_0 relationship

A simple algorithm to estimate D_0 from polarimetric measurements relates Z_{dr} to D_0 using a power law of the form $\hat{D}_0^{CPOL} = aZ_{dr}^b$ (Bringi et al. 2002; Gorgucci et al. 2002). The leading coefficient and exponent can be estimated using regressions on observed or simulated data (Jameson 1991; Brandes et al. 2004a, 2004b; Bringi et al. 2002; Vivekanandan et al. 2004). After estimating the uncertainty of Z_{dr} using (6), the $\hat{D}_0^{CPOL}$ uncertainty can be found by propagating the errors through the parameterization equation using

$$\mathrm{var}(\hat{D}_0^{CPOL}) = \mathrm{var}(Z_{dr})\left[\frac{\partial(\hat{D}_0^{CPOL})}{\partial Z_{dr}}\right]^2 = \mathrm{var}(Z_{dr})(abZ_{dr}^{b-1})^2. \quad (7)$$

Thus, the variance of $\hat{D}_0^{CPOL}$ is dependent on the magnitude and the variance of Z_{dr}. It should be noted that more complex regression relationships that include more variables will always have larger uncertainties due to increased random statistical errors but may lower bias errors substantially. Note that this analysis does not include errors due to sampling, attenuation, and, perhaps most important, the uncertainty in the regres-

sion relationship itself. The variances of all of these error sources contribute to the total variance and thus contribute to the uncertainty of the estimated D_0.

4. Observations

The presence of nonspherical raindrops in the rain leads to different attenuations along the horizontal and vertical polarization paths, which impacts the Z_{dr} estimate. The CPOL Z_{dr} estimates used in this study have been corrected for differential attenuation using a differential phase correction methodology described in detail by Bringi et al. (2001).

In addition to the purely statistical variations in D_0 discussed in section 2, there will be variations in D_0 due to the spatiotemporal sampling of the two radar systems. In the time domain, the scanning radar makes essentially instantaneous observations over the profiler site as it performs RHI scans every 10 min while the profiler requires 45 s of dwell time to collect one profile. The closest-in-time profiler observations to the RHI scans are analyzed in this study.

In the space domain, the scanning radar has a beamwidth of 0.95°, which yields a resolution volume with a vertical extent of about 500 m over the profiler site, while the 50-MHz profiler has 500-m range gates sampled every 300 m, and the 920-MHz profiler has 100-m range gates sampled every 100 m. In this study, the profiler vertical resolution is reduced to 500 m by averaging 920-MHz spectra in five consecutive range gates. The CPOL raw range resolution is 250 m and is averaged to 1 km by averaging Z_h and Z_{dr} over four consecutive range gates. The averaged radar pulse volumes from the two radars are comparable at approximately 10^8 m^3 at 2.5 km above the profiling radar. A cross-correlation analysis was performed using all simultaneous profiles of 100-m-vertical-resolution 920-MHz profiler and CPOL reflectivities to match the radar observations in height to account for Earth's curvature and ray bending between CPOL and the profiler site.

Note that the statistical errors of the power-law regression and the profiler retrieval errors are uncorrelated with the spatial errors associated with mismatches in the radar sample volumes, and they are also uncorrelated with the temporal errors associated with the evolution of the raindrop size distribution during the profiler dwell time. Thus, the variances from these four independent processes will be additive. This implies that the standard deviation of the differences between the profiling and scanning radar D_0 estimates are expected to be larger than any one of these error sources, including the statistical errors due to the power-law regression and the profiler retrieval uncertainties.

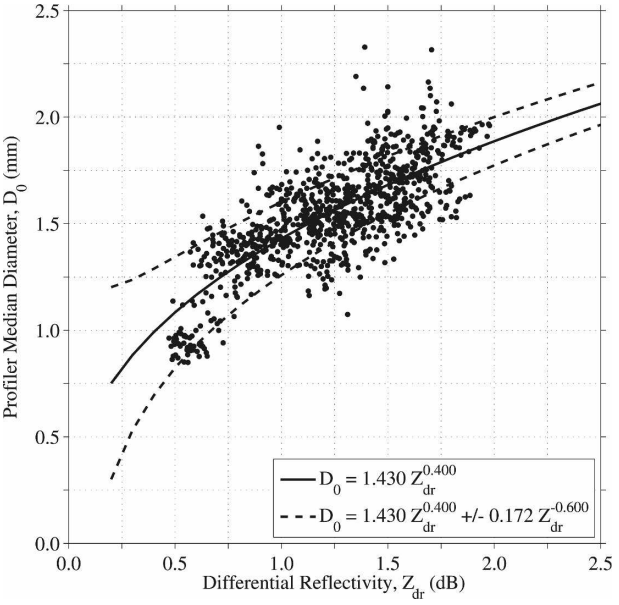

FIG. 1. Profiler median diameter $\hat{D}_0^{\text{prof}}$ (mm) vs CPOL differential reflectivity Z_{dr} (dB). The best-fit line $\hat{D}_0^{\text{CPOL}} = 1.43Z_{dr}^{0.40}$ is shown with the solid line. The uncertainties, shown with dashed lines, are calculated using $\hat{D}_0^{\text{CPOL}} = 1.43Z_{dr}^{0.40} \pm 0.172Z_{dr}^{-0.60}$. A total of 935 observations are from rain events on 31 Dec 2001 and 3 and 4 Jan 2002.

Three stratiform rain events are studied when simultaneous CPOL and profiler observations were available in December 2001 and January 2002. May et al. (2001) compared CPOL Z_{dr} and profiler-retrieved mean drop diameters for both rain and rain–hail mixtures, whereas this study analyzed only stratiform rain observations. The three events occurred during the monsoon season and consisted of leading convective events followed by large areas of stratiform rain with well-defined radar bright bands. Only the stratiform rain regime is analyzed in this study because of the increased spatial and temporal homogeneity of stratiform rain when compared with the leading convective rain regime and because the reduced turbulent broadening effects and longer temporal consistency during stratiform rain lead to more robust profiler retrievals.

a. Profiler D_0 versus CPOL Z_{dr}

For these three stratiform rain events, there were 935 simultaneous profiler and CPOL observations. Figure 1 shows the profiler-retrieved median raindrop diameter $\hat{D}_0^{\text{prof}}$ as a function of CPOL differential reflectivity Z_{dr}. Because the coefficients of a power-law expression of the form $\hat{D}_0^{\text{CPOL}} = aZ_{dr}^b$ are dependent on the regression method (Campos and Zawadzki 2000), the coefficients were estimated by minimizing the cost function

$$\chi^2 = \sum_{i}^{n=935} (\hat{D}_{0,i}^{\text{prof}} - aZ_{\text{dr},i}^{b})^2, \quad (8)$$

where the subscript i refers to each of the 935 profiler–CPOL data pairs. The estimated CPOL power-law expression was

$$\hat{D}_0^{\text{CPOL}} = 1.43Z_{\text{dr}}^{0.40}. \quad (9)$$

The uncertainty of the power-law $\hat{D}_0^{\text{CPOL}}$ expression was determined in section 3 and, assuming the largest estimated differential reflectivity uncertainty for the CPOL radar of 0.3 dB, the $\hat{D}_0^{\text{CPOL}}$ uncertainty is expressed as

$$\sigma(\hat{D}_0^{\text{CPOL}}) = \sigma(Z_{\text{dr}})(abZ_{\text{dr}}^{b-1}) = 0.172Z_{\text{dr}}^{-0.60}. \quad (10)$$

The derived power-law $\hat{D}_0^{\text{CPOL}}$ expression is shown in Fig. 1 as a solid line, and the uncertainty curves of $\hat{D}_0^{\text{CPOL}} \pm \sigma(\hat{D}_0^{\text{CPOL}})$ are shown as dashed lines. Note that $\sigma(\hat{D}_0^{\text{CPOL}})$ decreases with Z_{dr} with $\sigma(\hat{D}_0^{\text{CPOL}})$ equal to 0.17 and 0.11 mm when Z_{dr} is equal to 1 and 2 dB, respectively.

b. Differences between profiler and CPOL D_0

Although the mean difference between the profiler-retrieved and CPOL power-law regressed D_0s was minimized by the cost function using (8), the standard deviation of the differences between the two D_0 estimates was 0.16 mm. As mentioned previously, the standard deviation of the D_0 differences includes all uncertainty terms, including the radar retrieval uncertainties and the spatiotemporal variability of the raindrop size distribution. Since the standard deviation of the differences is less than the assumed profiler uncertainty of 0.25 mm, the profiler uncertainty must be less than 0.25 mm for these stratiform rain events, indicating that the profiler retrieval uncertainties for these events are smaller than the model studies. More analysis of profiler retrieval uncertainties is needed to quantify these errors more accurately.

5. Concluding remarks

In this study, the uncertainties of estimating the median raindrop diameter from the C-band polarimetric scanning radar (CPOL) near Darwin were investigated by propagating the measurement errors through a derived power-law regression. After estimating for this study that the differential reflectivity uncertainty had an upper limit of approximately 0.34 dB, the statistical uncertainty of the D_0 power-law regression was found to be a function of Z_{dr} but was less than 0.17 mm for D_0s greater than 1 mm.

To put these statistical uncertainties into context, the CPOL-derived D_0 estimates were compared with simultaneous profiler-derived D_0 estimates. While the CPOL observed the raindrops from the side, the vertically pointing profilers operating at 50 and 920 MHz observed the raindrops from the bottom. Analysis of profiler retrieval statistics suggests that the profiler-retrieved D_0 uncertainty is dependent on the amount of turbulent broadening occurring in the radar resolution volume. During stratiform rain, the turbulent broadening has a minimum value, and previous modeling studies suggest that the upper limit on the D_0 uncertainty should be approximately 0.25 mm.

In this study of three stratiform rain events, the standard deviation of the differences between profiler and polarimetric scanning radar D_0 estimates was 0.16 mm. Because this standard deviation of the difference includes both radar retrieval uncertainties and spatiotemporal variability of the raindrop size distribution, two conclusions can be drawn. First, the assumed upper limit of 0.25 mm on the profiler D_0 uncertainty is too large for this dataset of stratiform rain and must be less than 0.16 mm since the variances of the uncertainty sources are independent and additive. Second, the standard deviation of the differences is comparable to the statistical uncertainty of propagating the measurement errors through the D_0–Z_{dr} power-law regression and suggests that the power-law statistical uncertainty can be used to approximate the polarimetric D_0 uncertainties. Further analysis will be needed to quantify the observational and power-law regression uncertainties during convective rain, which has large temporal and spatial variability.

Acknowledgments. This work was supported in part by the NASA Tropical Rainfall Measuring Mission (TRMM) and Precipitation Measurement Mission (PMM) programs (Grant NNX07AN32G), in part by NOAA's contribution toward the NASA PMM program, and in part by the Australian Bureau of Meteorology Research Centre (BMRC). The Darwin 50-MHz profiler is owned and operated by the Australian Bureau of Meteorology (BOM). The Darwin 920-MHz profiler is owned by NOAA and is maintained and operated by BOM.

REFERENCES

Brandes, E. A., J. Vivekanandan, and J. W. Wilson, 1999: A comparison of radar reflectivity estimates of rainfall from collocated radars. *J. Atmos. Oceanic Technol.,* **16,** 1264–1272.

——, G. Zhang, and J. Vivekanandan, 2004a: Comparison of po-

larimetric radar drop size distribution retrieval algorithms. *J. Atmos. Oceanic Technol.,* **21,** 584–598.

——, ——, and ——, 2004b: Drop size distribution retrieval with polarimetric radar: Model and application. *J. Appl. Meteor.,* **43,** 461–475.

Bringi, V. N., and V. Chandrasekar, 2001: *Polarimetric Doppler Weather Radar*. Cambridge University Press, 636 pp.

——, T. D. Keenan, and V. Chandrasekar, 2001: Correcting C-band radar reflectivity and differential reflectivity data for rain attenuation: A self-consistent method with constraints. *IEEE Trans. Geosci. Remote Sens.,* **39,** 1906–1915.

——, G.-J. Huang, V. Chandrasekar, and E. Gorgucci, 2002: A methodology for estimating the parameters of a gamma raindrop size distribution model from polarimetric radar data: Application to a squall-line event from the TRMM/Brazil campaign. *J. Atmos. Oceanic Technol.,* **19,** 633–645.

Campos, E., and I. Zawadzki, 2000: Instrument uncertainties in *Z–R* relations. *J. Appl. Meteor.,* **39,** 1088–1102.

Doviak, R. J., and D. S. Zrnic, 1993: *Doppler Radar and Weather Applications*. Academic Press, 562 pp.

Gage, K. S., C. R. Williams, W. L. Ecklund, and P. E. Johnston, 1999: Use of two profilers during MCTEX for unambiguous identification of Bragg scattering and Rayleigh scattering. *J. Atmos. Sci.,* **56,** 3679–3691.

Gorgucci, E., V. Chandrasekar, B. N. Bringi, and G. Scarchilli, 2002: Estimation of raindrop size distribution parameters from polarimetric radar measurements. *J. Atmos. Sci.,* **59,** 2373–2384.

Gossard, E. E., 1988: Measuring drop-size distributions in clouds with a clear-air-sensing Doppler radar. *J. Atmos. Oceanic Technol.,* **5,** 640–649.

Jameson, A. R., 1991: Polarization radar measurements in rain at 5 and 9 GHz. *J. Appl. Meteor.,* **30,** 1500–1513.

Keenan, T. D., K. Glasson, F. Cummings, T. S. Bird, J. Keeler, and J. Lutz, 1998: The BMRC/NCAR C-band polarimeteric (CPOL) radar system. *J. Atmos. Oceanic Technol.,* **15,** 871–886.

——, L. D. Carey, D. S. Zrnić, and P. T. May, 2001: Sensitivity of 5-cm wavelength polarimetric radar variables to raindrop axial ratio and drop size distribution. *J. Appl. Meteor.,* **40,** 526–545.

Lucas, C., A. D. MacKinnon, R. A. Vincent, and P. T. May, 2004: Raindrop size distribution retrievals from a VHF boundary layer radar. *J. Atmos. Oceanic Technol.,* **21,** 45–60.

May, P. T., and T. D. Keenan, 2005: Evaluation of microphysical retrievals from polarimetric radar with wind profiler data. *J. Appl. Meteor.,* **44,** 827–838.

——, A. R. Jameson, T. D. Keenan, and P. E. Johnston, 2001: A comparison between polarimetric radar and wind profiler observations of precipitation in tropical showers. *J. Appl. Meteor.,* **40,** 1702–1717.

Rajopadhyaya, D. K., P. T. May, R. C. Cifelli, S. A. Avery, C. R. Williams, W. L. Ecklund, and K. S. Gage, 1998: The effect of vertical air motions on rain rates and median volume diameter determined from combined UHF and VHF wind profiler measurements and comparisons with rain gauge measurements. *J. Atmos. Oceanic Technol.,* **15,** 1306–1319.

——, S. A. Avery, P. T. May, and R. C. Cifelli, 1999: Comparison of precipitation estimation using single- and dual-frequency wind profilers: Simulations and experimental results. *J. Atmos. Oceanic Technol.,* **16,** 165–173.

Ralph, F. M., 1995: Using radar-measured radial vertical velocities to distinguish precipitation scattering from clear-air scattering. *J. Atmos. Oceanic Technol.,* **12,** 257–267.

Sato, T., D. Hiroshi, H. Iwai, I. Kimura, S. Fukao, M. Yamamoto, T. Tsuda, and S. Kato, 1990: Computer processing for deriving drop-size distributions and vertical air velocities from VHF Doppler radar spectra. *Radio Sci.,* **25,** 961–973.

Schafer, R., S. A. Avery, P. T. May, D. Rajopadhyaya, and C. Williams, 2002: Estimation of drop size distributions from dual-frequency wind profiler spectra using deconvolution and a nonlinear least squares fitting technique. *J. Atmos. Oceanic Technol.,* **19,** 864–874.

Seliga, T. A., and V. N. Bringi, 1976: Potential use of the radar reflectivity at orthogonal polarizations for measuring precipitation. *J. Appl. Meteor.,* **15,** 69–76.

Ulbrich, C. W., 1983: Natural variations in the analytical form of the raindrop size distribution. *J. Climate Appl. Meteor.,* **22,** 1764–1775.

Vivekanandan, J., G. Zhang, and E. Brandes, 2004: Polarimetric radar estimators based on a constrained gamma drop size distribution model. *J. Appl. Meteor.,* **43,** 217–230.

Wakasugi, K., A. Mizutani, M. Matsuo, S. Fukao, and S. Kato, 1986: A direct method for deriving drop-size distribution and vertical air velocities from VHF Doppler radar spectra. *J. Atmos. Oceanic Technol.,* **3,** 623–629.

Williams, C. R., 2002: Simultaneous ambient air motion and raindrop size distributions retrieved from UHF vertical incident profiler observations. *Radio Sci.,* **37,** 1024, doi:10.1029/2000RS002603.

——, A. Kruger, K. S. Gage, A. Tokay, R. C. Cifelli, W. F. Krajewski, and C. Kummerow, 2000: Comparison of simultaneous rain drop size distributions estimated from two surface disdrometers and a UHF profiler. *Geophys. Res. Lett.,* **27,** 1763–1766.